

## Development of 77 GHz-1 MW ECRH system for LHD

Hiromi TAKAHASHI<sup>1)</sup>, Takashi SHIMOZUMA<sup>1)</sup>, Shin KUBO<sup>1)</sup>, Yasuo YOSHIMURA<sup>1)</sup>, Hiroe IGAMI<sup>1)</sup>, Satoshi ITO<sup>1)</sup>, Sakuji KOBAYASHI<sup>1)</sup>, Yoshinori MIZUNO<sup>1)</sup>, Yasuyuki TAKITA<sup>1)</sup>, Takashi MUTOH<sup>1)</sup>, Tsuyoshi KARIYA<sup>2)</sup>, Ryutaro MINAMI<sup>2)</sup>, Tsuyoshi IMAI<sup>2)</sup>

<sup>1)</sup> National Institute for Fusion Science

<sup>2)</sup> Plasma Research Centre, University of Tsukuba, Tsukuba 305-8577, Japan

In the Large Helical Device (LHD), the development of new 77 GHz gyrotrons of the design value of more than 1 MW for 5 s and 300 kW for CW have started from 2006 as the joint program between NIFS and University of Tsukuba. The replacement of the existing gyrotrons by the 77 GHz-1 MW tubes is in progress. Two 1 MW tubes have been installed in LHD up to now. We have also finished the arrangement of the peripheral components including the transmission line. We have attained the operation of 0.86 MW/ 1.1 s and 0.76 MW/ 5 s for each 77 GHz gyrotron.

Keywords: ECRH, gyrotron, matching optics unit, steady state operation, LHD

### 1. Introduction

Electron cyclotron resonance heating (ECRH) is one of the most promising heating methods for fusion plasmas due to its higher power density and lower risk for neutron activation. From the view point of plasma control, ECRH also plays a key role as a control knob for local plasma parameters by local heating or toroidal current drive with a high spatial resolution [1]. Thus, it is substantially important to develop gyrotrons with a capability of high-power generation and long-time oscillation for effective utilization of ECRH as a plasma control knob and extension of parameter regime of long-time sustained plasma.

In the Large Helical Device (LHD) [2], the enhancement of the output power per gyrotron was planned to enlarge the plasma operational regime and the replacement of the existing gyrotrons to high-power ones is progressed. 8 sets of gyrotron are operated and the total injection power of ECRH to plasma is less than 2 MW. We will replace all these gyrotrons to 1 MW-ones and set ultimate goal as the total injection power of 5 MW. The oscillation frequencies of these 1 MW-gyrotrons are selected as 77 or 154 GHz and are different from those of the gyrotrons already installed in LHD. The frequency of 77 GHz is resonant with the fundamental electron cyclotron resonance layer on axis of the standard configuration of LHD, which shows good plasma confinement [3], so a higher electron temperature on the axis and a higher peaking factor of the temperature profile than that obtained previously are expected. Moreover, these gyrotrons have the capability of 300 kW-continuous oscillation, thus the gyrotron will contribute to the expansion of the parameter regime of

long-time-sustained plasma. LHD has a capability of long-pulse operation [4] of high temperature/density plasma due to the superconducting coil system and various heating source. Therefore, LHD can be said one of the most appropriate devices for extrapolation to steady-state fusion reactor in terms of the size and the feature.

In this paper, we show the progress of the installation of the 77 GHz 1 MW-gyrotrons for LHD. The paper is organized as follows. In section 2, the ECRH system in LHD is described. Section 3 deals the characteristics of the 1 MW-gyrotrons and the peripheral components. In Section 4, the results of the short/long pulse operation and the achieved operational regime are shown. Final conclusions are presented in section 5.

### 2. ECRH system in LHD

LHD is the largest heliotron device with  $R = 3.9$  m,  $a = 0.6$  m, which has the pole number of 2 and the toroidal period of 10. The heliotron configurations are produced by a set of helical winding coils and three sets of poloidal field coils, which are all superconducting magnet. Therefore the steady-state formation of magnetic configuration and plasma sustainment has been realized. The magnetic field on axis is  $\sim 2.9$  T.

In LHD, ECRH system with 8 sets of gyrotron, which frequencies are 77 (Toshiba Electron Tubes & Devices, TETD), 82.7 (Gycom), 84 (Gycom) and 168 GHz (TETD), have been operated for preionization and plasma heating [5]. Among them, the 77-GHz gyrotrons has been newly installed since the experimental campaign of 2007. These are the collector-potential-depression (CPD) type gyrotrons [6] for high efficiency operation

excluding those of 82.7 GHz. One of the 84 GHz gyrotron has the capability of continuous-wave (CW) oscillation and that is mainly used for steady-state plasma experiments [7]. The type of magnetron injection gun (MIG) is triode for TETD tubes and diode for Gycom tubes, respectively. These gyrotrons are set at the heating equipment room next to the LHD hall. Each ECRH system is composed of gyrotron tube, power supply for gyrotron, matching optics unit (MOU), waveguides, miter bends, arc detectors, dummy load, waveguide switch, antenna and the other components. The millimetre wave power is transmitted to LHD through the corrugated waveguides with the inner diameter of 31.75 mm or 88.9 mm after transformation of the beam to  $HE_{11}$  mode at the MOU and injected to the plasma using injection antennas. One of the antennas is mirror type antenna consisted of one focusing mirror and one steering mirror. The other is waveguide antenna used for CW gyrotron. The transmission efficiency of ECW is about 60-95 % depending on the number of the miter bend, the length of the transmission line, and the other factors.

### 3. Configuration of 1 MW-Gyrotron

Since July 2007, the installation of the 1 MW-gyrotrons designed by TETD has progressed in LHD and two 1 MW-tubes have been operated in the present circumstance. The design of the gyrotron and the configuration with the MOU are shown in Tab I and Fig. 1. The gyrotron type is CPD and the gun is a triode configuration cathode for controllability. 6 sweep coils are set around the collector and a triangular current of 1.9 Hz is applied to the coils to change the injection point of the spent electron beam temporally in order to avoid the local heat accumulation.  $TE_{18,6}$  is selected as the cavity mode taking the cathode configuration, the radio frequency (RF) power loss on the inner wall, matching with the mode converter into consideration. RF beam is projected from output window after the shaping by 4 copper mirrors in the gyrotron. A chemical-vapor-deposition (CVD) diamond disc with high thermal conductivity and low dielectric constant is used for the projection window so a higher output/ longer pulse operation is realized. Moreover, the diamond window allows the projection of RF beam with  $TEM_{00}$  mode leading to less power loss in the shaping to  $HE_{11}$  mode at the MOU. The diamond disc is also used for injection window to LHD.

A MOU is set as illustrated in Fig. 1. The MOU mirror system consists of 2 copper mirrors with the major axis of 100 mm and the minor axis of 80 mm. A phase distribution of an RF beam is corrected by these mirrors. The mirror surface was designed by the convergence calculation for the height of the bumpy on the mirror

TAB I Design of 77 GHz gyrotrons

Items	Design
Frequency	77 GHz
Power/ Pulse length	1.0 MW/ 5.0s, 0.3 MW/ CW (#1) 1.2 MW/ 5.0s, 0.3 MW/ CW (#2)
Beam Current	$\leq 50$ A
Cavity mode	$TE_{18,6}$
MIG type	Triode
Collector type	Collector Potential Depression
Output window	CVD Diamond

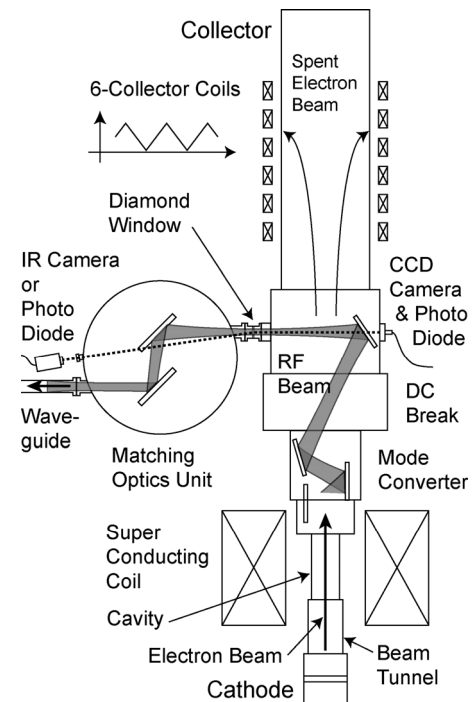


Fig.1 The gyrotron configuration with the MOU.

corresponding to the phase difference between the initial phase distribution and the goal one, which was calculated from the inverse diffraction for  $HE_{11}$  mode at MOU projection port. The design value of transmission efficiency of the MOU is 98.8 %. The alignment of the RF beam was done by the adjustment of these two mirrors and the gyrotron final mirror. An arcing in the MOU is monitored through the sapphire window by the arc detector (photo diode) set at the ICF 70 port located on the same surface of the MOU projection port. The temperature profile of the diamond window during an operation is also monitored using an IR camera through the port.

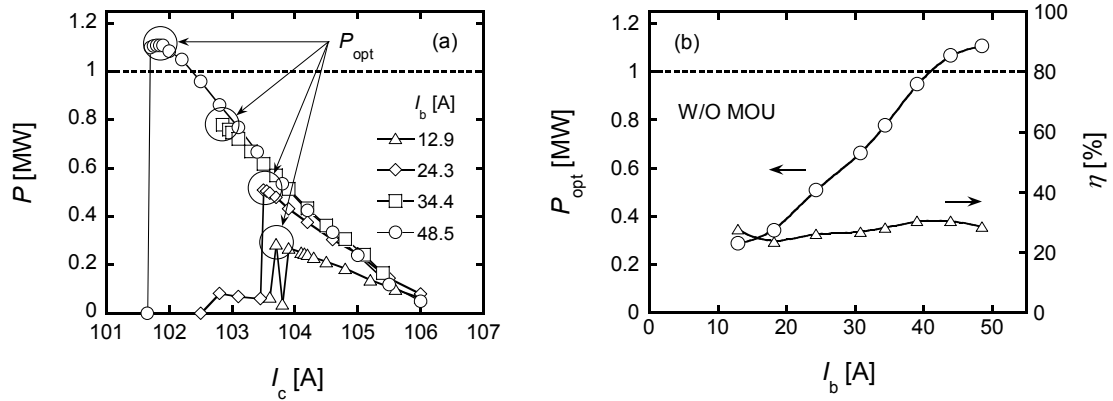


Fig.2 The dependence of (a) the output power on the coil current, (b) the maximum output power and the oscillation efficiency on the electron beam current.

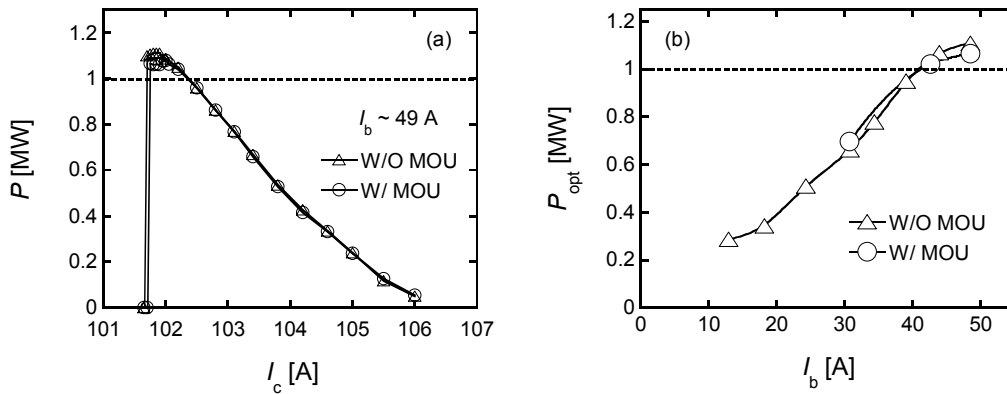


Fig. 3 The dependence of (a) the output power on the coil current and (b) the maximum output power on beam current W/, W/O the MOU. The operation of 1 MW output was attained even with the MOU.

#### 4. Short and long pulse operations

After the arrangement of the cooling system for the gyrotron components, we started the short-pulse test. In this operation, the output power was monitored using short-pulse dummy load connected to the projection port of the gyrotron. Figure 2 shows the dependence of (a) the output power  $P$  on the coil current of the superconducting magnet at the cavity  $I_c$ , (b) the maximum output power  $P_{opt}$  and the oscillation efficiency  $\eta$  on the electron beam current  $I_b$  for #1 77 GHz-gyrotron. In this operation, the dummy load was evacuated to  $\sim 10^{-4}$  Torr and the pulse length of the gyrotron oscillation was set for 3 ms. The oscillation region of the operating mode elongated to the lower magnetic field side with  $I_b$  increasing and  $P = 1.1$  MW was achieved at  $I_b = 48.5$  A. The maximum oscillation efficiency of 30.5 % was confirmed at  $I_b = 43.9$  A. We also checked the transmission efficiency of the MOU. Figure 3 shows the dependence of (a)  $P$  on  $I_c$  and (b)  $P_{opt}$  on  $I_b$  W/, W/O the MOU for #1 77 GHz-gyrotron. It was confirmed that the power loss due

to the MOU was small and the 1 MW output was attained even with the MOU. Eventually, we performed the operation of 1.05 MW/ 4 ms.

After 1 MW test for short pulse, we proceeded to a long pulse operation. The conditioning in the long pulse operation was performed using CW-dummy loads. A pre-dummy load is set upon each CW-dummy load in order to absorb reflected waves from the CW-dummy load. The output power from the gyrotron in the long-pulse operation was evaluated as the sum of the absorption power at CW- and pre-dummy load. Figure 4 shows the progress of the extension of the power and the pulse length for #1 ((a), (b)) and #2 gyrotron ((c), (d)), (e) the operational regime and its present boundary in power vs. pulse length until October 16, 2008. In Fig. 4 (e), the open circles and the open squares represent the attained operation regime for #1 and #2 gyrotron, respectively. We operated the gyrotrons for  $\sim 200$  hours in the cumulative operational time. Up to now, we attained the operation of 860 kW/ 1.1 s, 500 kW/ 5.0s for #1 gyrotron and 760 kW/

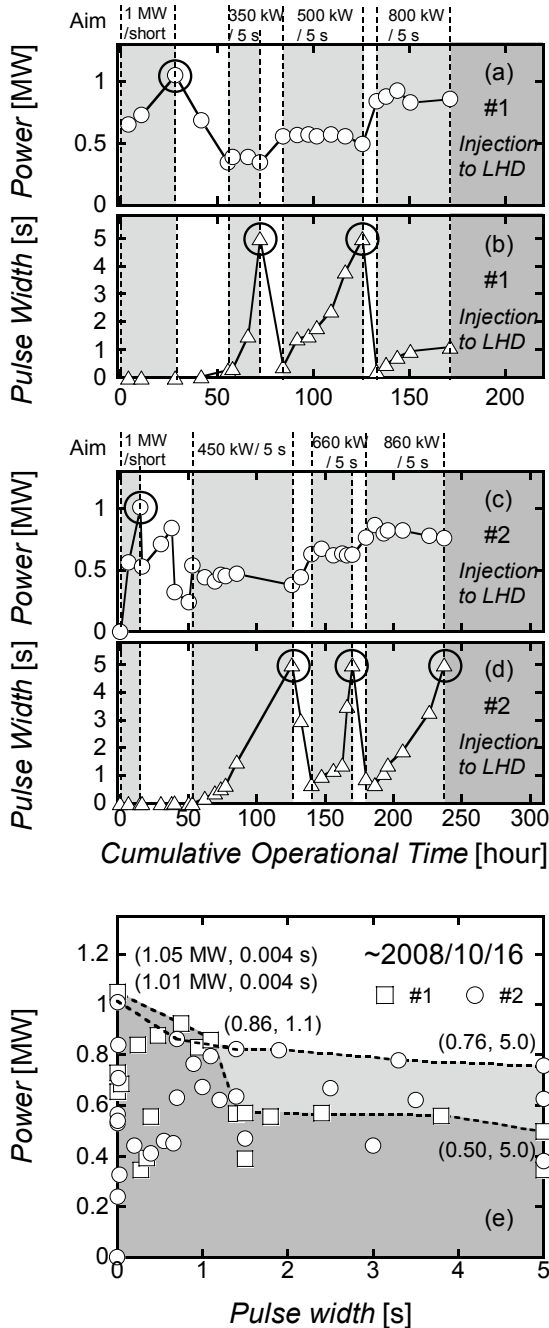


Fig. 4 (a)-(d) the progress of power and the pulse length, (e) the attained operational regime and its present boundary.

5.0 s for #2 one. Finally, we show the typical oscillation of high power output for 5.0 s. Figure 5 shows the time evolution of (a) collector, body and anode voltage  $V_C$ ,  $V_B$ ,  $V_A$ , (b) beam and anode current  $I_b$ ,  $I_A$  and (c) output power  $P$ . Although the output power exceeded 800 kW at the beginning of the oscillation, it decreased gradually with the beam current decrease. We now try to apply a temporal heater boosting with preprogram to compensate the beam current decrease.

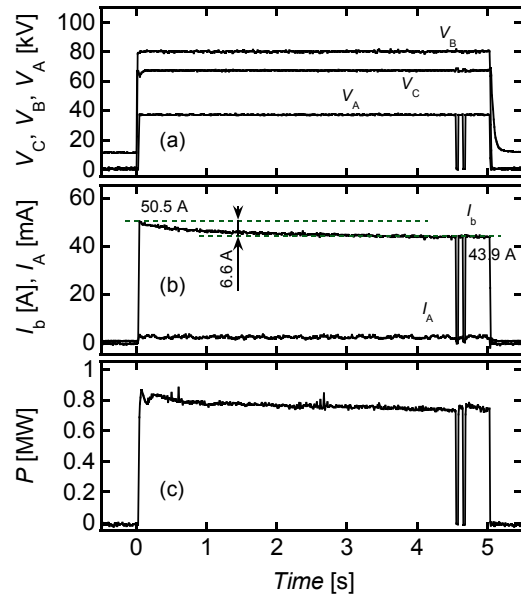


Fig. 5 The time evolution of (a) collector, body and anode voltage, (b) beam and anode current and (c) output power.

**5. Summary**

77 GHz gyrotron of the design value 1 MW/ 5 s and 300 kW/ CW was newly installed in LHD and the arrangement of the peripheral component has already done. We have attained the operation of 0.86 MW/ 1.1 s and 0.76 MW/ 5 s for each 77 GHz gyrotron. In future work, we will extend the operational regime to 1 MW/ 5 s or 1.2 MW/ 5s and 300 kW/ CW. In parallel to that, we start the installation of second 77 GHz gyrotron (1.5 MW/ several sec., 300 kW/ CW), which has already developed.

**Acknowledgment**

We wish to acknowledge useful discussions with Professor K. Sakamoto. We are grateful to Dr. Y. Mitsunaka for the development of the gyrotron. This work was supported by NIFS grants, ULRR501, ULRR503, ULRR512, ULRR514 and ULRR518.

**References**

- [1] V. Erckmann and U. Gasparino, Plasma Phys. Control. Fusion **36**, 1869 (1994).
- [2] O. Motojima *et al.*, Nucl. Fusion **45**, No 10, S255 (2005).
- [3] H. Yamada *et al.*, Nucl. Fusion **41**, No 7, 901 (2001).
- [4] T. Mutoh *et al.*, Nucl. Fusion **47**, No 9, 1250 (2007).
- [5] S. Kubo *et al.*, Plasma Phys. Control. Fusion **47**, No 5A, A81 (2005).
- [6] K. Sakamoto *et al.*, Phys Rev. Lett. **73**, 3532 (1994).
- [7] T. Shimozuma *et al.*, Fusion Eng. Des. **53**, 525 (2001).
- [8] T. Notake *et al.*, Plasma Phys. Control. Fusion **47**, 531 (2005).